Chemical Science

ROYAL SOCIETY OF CHEMISTRY

EDGE ARTICLE

View Article Online
View Journal | View Issue

Cite this: *Chem. Sci.*, 2024, **15**, 19583

All publication charges for this article have been paid for by the Royal Society of Chemistry

Simultaneous generation of hydroxyl and hydrogen radicals from H^+/OH^- pairs caused by water–solid contact electrification†

Fengjie Chen,‡[a] Jingde Wu,‡[b] Dou Wang,[c] Yu Xia,[a] Qingyuan Song,[d] Ying Liang,[a] Pu Wang,[a] Bolei Chen, *[ad] Yong Liang,[a] Yongguang Yin,[d] Yawei Wang,[ad] Maoyong Song[d] and Guibin Jiang[d]

Water–solid contact electrification is a common physical phenomenon involving interfacial electron and ion transfer, recently discovered to trigger unique redox reactions. Here, we demonstrate the generation of both hydroxyl and hydrogen radicals when water contacts SiO_2. The coexistence of hydroxyl and hydrogen radicals is confirmed by simultaneous nitrate reduction and nitrite oxidation during the contact. Increased density of hydroxyl groups on the SiO_2 surface enhances its surface electronegativity before the contact, as well as boosting charge transfer and radical generation during the contact. We propose that the simultaneous generation of hydroxyl and hydrogen radicals originates from electron gain and loss between hydroxide anions in water and hydrogen cations adsorbed on the solid surface, which are ion pairs separated by the interfacial electric field. This discovery advances our understanding of redox processes induced by contact electrification.

Received 14th September 2024
Accepted 4th November 2024

DOI: 10.1039/d4sc06227b

rsc.li/chemical-science

Introduction

Water–solid contact electrification is relevant to a variety of mechanochemical, environmental, and catalytic processes, as well as playing a crucial role in chemical synthesis technology and energy devices.[1–6] There is growing evidence suggesting that this physical stimulus would result in transfer of both electrons and ions between water and a solid surface,[7,8] influencing oxidation and reduction reactions at the aqueous interface.[9–11] Our previous work demonstrated that the contact between aqueous microdroplets and the SiO_2 substrate causes the spontaneous generation of reactive oxygen species (ROS) in the microfluidic channel.[12] The presence of hydroxyl groups on the solid surface and their hydrogen bonding network play key roles in the oxidation chemical processes.[10,13] Other researchers reported that the contact between water and polytetrafluoroethylene (PTFE) particles in bulk suspension catalyses ROS generation from hydroxide anions (OH^-) under ultrasonication.[3,6] Moreover, recent work found that the water–PTFE contact electrification can also lead to continuous reduction of nitrogen (N_2) absorbed on a solid surface by bubbling the gas into the bulk aqueous suspension.[14] These findings imply that complex reaction pathways exist during water–solid contact. Notably, similar spontaneous oxidation and reduction processes, or even simultaneous redox reactions, can be caused by the strong electric field at the surface of the sprayed water microdroplets.[15–20] However, it is not possible to apply the reaction mechanism in microdroplets to explain the observation during water–solid contact, since the electric field and charge transfer behaviour at the water–solid interface are completely different compared to the water–gas interface. In what follows, we present evidence for the simultaneous oxidation and reduction reactions that occurred during water–SiO_2 contact electrification. We show that the hydrogen radical and hydroxyl radical act as the reductant and oxidant, respectively, triggering opposite but simultaneous redox reactions. Considering that water loses electrons and solids gain electrons during contact electrification, OH^- ions in water and H^+ absorbed on SiO_2 may work as electron donors and acceptors, respectively, and thus become sources of the radicals during the contact.

[a]*Hubei Key Laboratory of Environmental and Health Effects of Persistent Toxic Substances, School of Environment and Health, Jianghan University, Wuhan, 430056, China*

[b]*School of Environment, Hangzhou Institute for Advanced Study, UCAS, Hangzhou, 310000, China*

[c]*State Key Laboratory for Managing Biotic and Chemical Treats to the Quality and Safety of Agro-products, Institute of Agro-product Safety and Nutrition, Zhejiang Academy of Agricultural Science, Hangzhou, 310012, China*

[d]*State Key Laboratory of Environmental Chemistry and Ecotoxicology, Research Center for Eco-Environmental Sciences, Chinese Academy of Sciences, Beijing, 10085, China. E-mail: blchen@rcees.ac.cn*

† Electronic supplementary information (ESI) available: Additional data and experimental details. See DOI: https://doi.org/10.1039/d4sc06227b

‡ These authors contributed equally to this work.

Results and discussion

An ideal water–solid contact model was constructed based on SiO_2 microspheres with a diameter of 60 μm sealed in a home-made chamber as shown in Fig. 1A. The SiO_2 microspheres were chosen as the solid phase material in order to create a large contact surface area to initiate a strong enough chemical process to facilitate subsequent detection.[10] We applied water-carrying argon gas contact with SiO_2 to minimize the effect of bulk water on the reaction process at the contact interface. The use of argon excluded the influence of reactive gases such as oxygen and ozone in our reaction system. Notably, the water-carrying argon gas was obtained by bubbling the gas through DI water, which was deionized reagent-grade with a resistivity larger than 18 MΩ cm. A ROS-sensitive probe (2′,7′-dichlorodihydrofluorescein diacetate, DCFH-DA) and a reductive species-sensitive water-soluble probe (resazurin) were used to detect the generation of ROS and reductive species at the water–solid interface, respectively (shown in Fig. S1†). The fluorescence probes dissolved in the source water were carried by argon gas to the SiO_2 surface to react with possible ROS and reductive species. After 2 hours of continuous contact between H_2O and SiO_2 microspheres, the SiO_2 microspheres were placed on a glass slide for fluorescence microscopy measurement. Typically, red fluorescence emission was observed on the SiO_2 surface under 570 nm laser excitation (as shown in Fig. 1B), while green fluorescence emission was observed on the surface of the SiO_2 micro-sphere under 488 nm laser excitation (as shown in Fig. 1C). To rule out the artificial error caused by the fluorescence measurement, we compared the fluorescence intensity on the SiO_2 surface before and after the contact. As shown in Fig. S2,† the fluorescence emission from the SiO_2 microsphere surface can hardly be observed before the water–solid contact occurred. These results indicated that both ROS and reductive species can be generated during contact electrification. Moreover, we carried out electron spin resonance spectroscopy (ESR) to identify the radicals generated during the contact. As shown in Fig. 1D, the signal from hydrogen radicals, highlighted by the red "*" symbol, was observed on the surface of SiO_2 microspheres after the contact. However, four peaks with a 1 : 2 : 2 : 1 intensity ratio (highlighted by the green "•" symbol) appeared, which can be attributed to hydroxyl radicals.[21,22] This result reveals that the response signals of fluorescence probes observed in Fig. 1B and C can be attributed to the generation of hydrogen and hydroxyl radicals, respectively.

In order to elucidate the simultaneous generation of hydroxyl and hydrogen radicals during the contact process, we contacted moist argon gas carrying both sodium nitrate and sodium nitrite with SiO_2 microspheres and analyzed the reaction products. The ion chromatography measurements were carried out immediately after the contact occurred between water and SiO_2. By comparing the NO_3^-/NO_2^- ratio before and after the contact shown in Fig. 2A, we found that the reduction of nitrate or oxidation of nitrite may happen.[23] And the nitrite and nitrate generation during water–solid contact increased with the increase of the flow rate of argon gas (Fig. S3†). Notably, we employed ^{15}N isotopically labeled sodium nitrate and normal sodium nitrite as starting reactants to distinguish their products during the contact.[24] Their mass spectra are displayed in Fig. S4.† After the contact between water and SiO_2 occurred, the ^{15}N isotopically labeled nitrite cation ($^{15}NO_2^-$) was observed at m/z at 47, while the generation of the nitrate cation (NO_3^-) was confirmed by the peak at m/z 62 (shown in Fig. 2B). The peaks at m/z 63 and m/z 46 can be attributed to incompletely reacted starting reactants. By comparing the changes in the mass spectra before and after the water–solid contact, it is clear that ^{15}N isotope-labeled nitrite and normal nitrite are generated spontaneously and simultaneously during the contact process.

To further understand the above redox reactions, we analyze the oxidation and reduction during the contact process

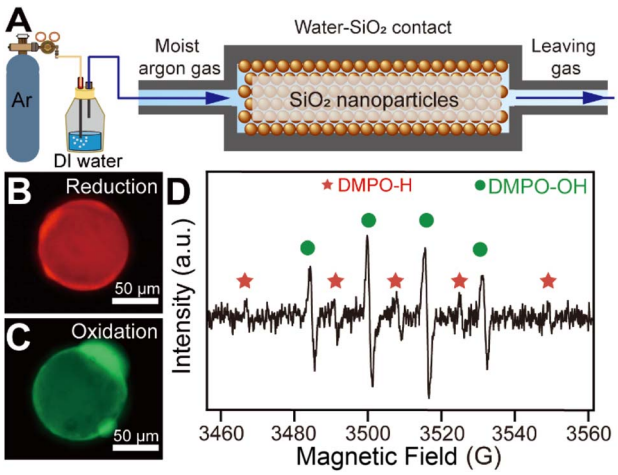

Fig. 1 (A) Schematic representation of the experimental setup. (B) A typical fluorescence microscopy image of reductive species generated on the surface of a SiO_2 microsphere. (C) A typical fluorescence microscopy image of ROS generated on the surface of a SiO_2 microsphere. (D) Corresponding ESR result for SiO_2 micro-spheres after contacting with water-carrying argon gas.

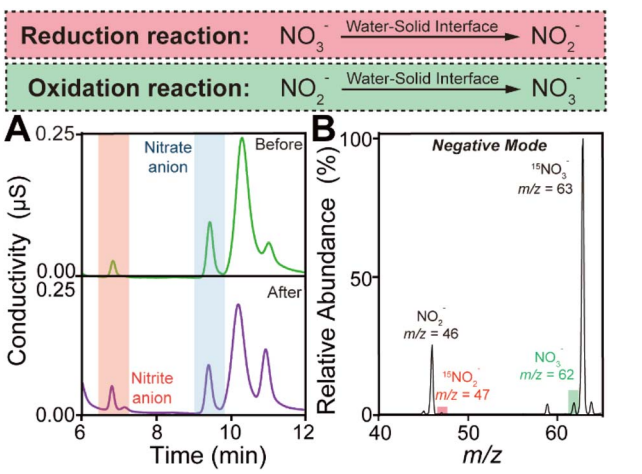

Fig. 2 (A) Ion chromatography showing the transformation of NO_2^- and NO_3^- before and after the water–solid contact. (B) Mass spectrum in negative mode showing the oxidation of NO_2^- and the reduction of $^{15}NO_3^-$.

separately. When moist argon gas containing $NaNO_3$ was contacted with SiO_2, ion chromatography measurements indicated that nitrate was converted to nitrite as shown in Fig. S5.† The corresponding mass spectra obtained in the negative and positive modes are displayed in Fig. S6A and B.† The peak observed in negative mode at m/z 46 further confirms the reduction of $NaNO_3$ during the contact. Observation of the peak at m/z 63 could be attributed to the intermediate product produced in the reduction of NO_3^- by hydrogen radicals ($NO_3^- + {}^{\bullet}H \rightarrow NO_3H^{\bullet -}$).[25] Then the $NO_3H^{\bullet -}$ further reacted with hydrogen radicals to generate NO_3^- ($NO_3H^{\bullet -} + {}^{\bullet}H \rightarrow NO_2^{\bullet -} + H_2O$). Furthermore, in the positive mode, the peak at m/z 36 suggests that the hydroxyl radical is generated from an ion in the water during the contact process, regardless of whether the ion is OH^- or the water radical cation.[20,26] Replacing water with heavy water (D_2O) gave the corresponding mass spectrum in the negative mode of deuterated ions as shown in Fig. S7.† Similarly, the oxidation of NO_2^- was confirmed by ion chromatography measurements and mass spectra shown in Fig. S8A and B.† Notably, in negative mode, the peak at m/z 63 was hardly observed during the oxidation process caused by water–solid contact. We believe that this result provides further evidence for the participation of hydrogen radicals in the reduction reaction caused by contact electrification. Moreover, in positive mode, we calculated the relative peak intensities at m/z 36 representing the hydroxyl radical generation when using the mass spectral peak of the hydrated sodium ion as an internal standard. The relative peak intensity at m/z 36 observed during the oxidation of NO_2^- is lower than that obtained during the reduction of NO_3^-. This result further confirmed the generation of the hydroxyl radical caused by the water–solid contact process and induced the NO_2^- oxidation ($NO_2^- + 2{}^{\bullet}OH \rightarrow NO_3^- + H_2O$). These observations are in good agreement with the ESR measurements displayed in Fig. S9.† Considering the coexistence of hydroxyl and hydrogen radicals, we believe that both radicals are generated by the gain and loss of electrons from ion pairs, which are separated by the electric double layer at the water–solid interface. Importantly, based on the common sense that electrons are transferred from water to SiO_2 during contact electrification, we conjectured that the generation of hydroxyl radicals originates from the process of electron loss by the OH^- in water, while the production of hydrogen radicals is attributed to the process of electron gain by the H^+ adsorbed on the surface of the solid.

To confirm our conjecture, we obtained SiO_2 microspheres with different surface electronegativity by varying the hydroxyl group density on the solid surface as shown in Fig. 3A and S10.† We believe that microspheres with high surface hydroxyl group density can adsorb more H^+ when water is in contact with the solid. Fig. 3B reveals that electron transfer caused by water–solid contact electrification increased with increasing surface hydroxyl density. This result could be attributed to more H^+ which acts as an electron acceptor during the contact, while OH^- in water is considered to be in excess as an electron donor. Furthermore, the ESR measurements and ion chromatography quantitative analysis, as shown in Fig. 3C and D, indicate that the simultaneous generation of hydroxyl and hydrogen radicals was enhanced by increasing the charge transfer during contact

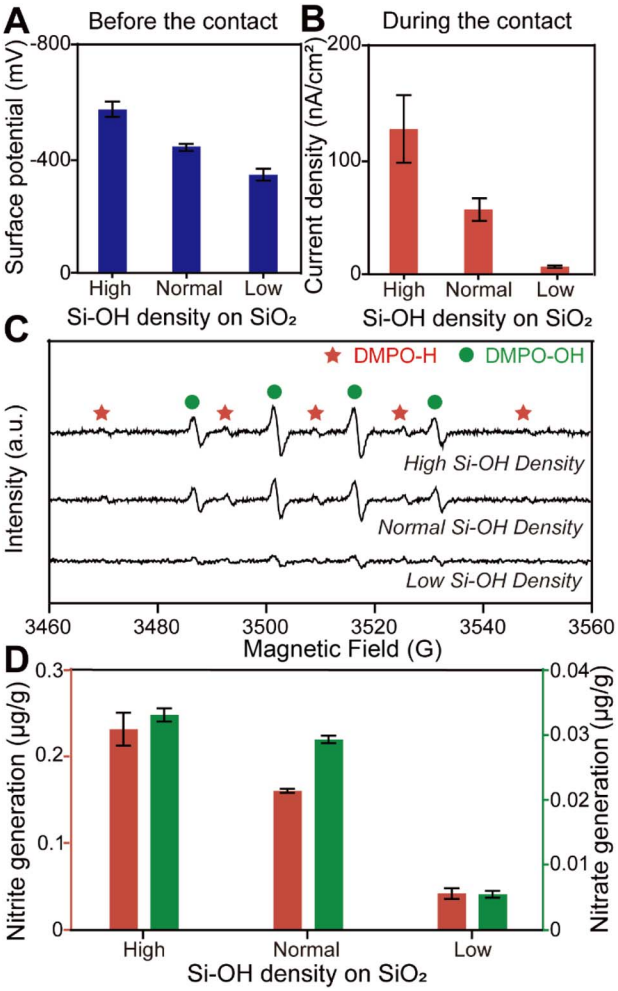

Fig. 3 (A) Surface potential of SiO_2 samples with different hydroxyl group density before the contact measured by Kelvin probe force microscopy (KPFM). (B) The corresponding current density of SiO_2 samples with different hydroxyl group density during the contact. (C) The corresponding ESR spectra of SiO_2 samples after the contact process. (D) Nitrite and nitrate generation during water–solid contact depending on the density of hydroxyl groups on the SiO_2 surface.

electrification. We believe that these findings provide evidence for our hypothesis that H^+ from the stem layer and OH^- in the diffusion layer at the water–solid interface are responsible for

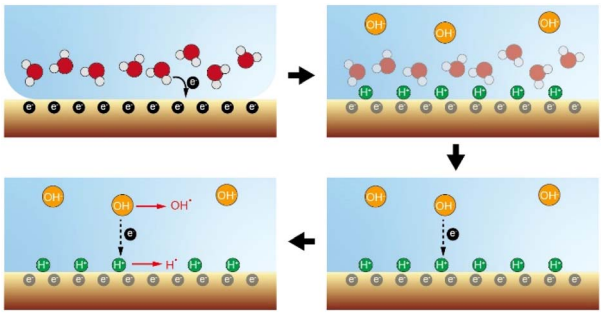

Fig. 4 Proposed mechanism for simultaneous generation of hydrogen and hydroxyl radicals caused by water–solid contact electrification.

the simultaneous reduction and oxidation under the physical stimuli of the contact.

As shown in Fig. 4, a possible reaction pathway was constructed to describe the simultaneous generation of hydrogen and hydroxyl radicals when water–solid contact occurs. Firstly, electrons are transferred from water to the solid surface during the initial stage of the contact (contact electrification), leading to an increase in the electronegativity of the solid surface. Secondly, the solid surface absorbs H^+ ionized from the acidic hydroxyl functional groups, which in turn forms a double electric layer. Notably, although each material carries a net charge of either positive or negative polarity, their surface supports a random "mosaic" of oppositely charged regions of nanoscopic dimension.[27,28] We speculate that the non-uniform distribution of these charges during water–solid contact can cause enrichment of H^+ in some regions of the solid surface, which in turn leads to the formation of a strong electric field directly between H^+ in the stem layer and OH^- in the diffusion layer, causing electrons to be stripped from OH^- and transfer toward the adsorbed H^+ on the solid surface. Simultaneously, a small portion of OH^- loses their electrons and form hydroxyl radicals, while H^+ gains electrons and generates hydrogen radicals. Finally, the hydrogen and hydroxyl radicals together mediate the interfacial redox chemical processes.

Conclusions

In conclusion, we report the simultaneous and spontaneous oxidation and reduction reactions when the contact occurred between water and the SiO_2 surface. We have provided a series of evidence showing that the redox reactions observed during the water–solid contact are triggered by hydroxyl and hydrogen radicals. Importantly, the coexistence of hydroxyl and hydrogen radicals suggests that their generation can be attributed to electron gain and loss of OH^-/H^+ ion pairs, which are separated by an electric field at the water–solid interface. We believe that our hypothesis is applicable to explain the redox processes in sprayed microdroplets, as well as the observation at the water–oil interface. Moreover, these findings might provide new insight into understanding the redox chemistry in the atmosphere under dark conditions.

Data availability

All data utilized in the manuscript have been uploaded to the Science Data Bank repository and are available at **https://www.scidb.cn/s/rQN7Rr**.

Author contributions

F. C. and J. W. conceptualized the specific research in close consultation with B. C., who conceived the overall project and acquired necessary funding. D. W. and Y. X. developed and implemented the water–solid model. Q. S. and Y. L. conducted fluorescence experiments and image segmentation. F. C. conducted the remaining experiments. P. W., Y. L., Y. Y., Y. W., M. S. and G. J. participated in the discussion of the experiments and related results. The manuscript was written through contributions of all authors. All authors have given approval to the final version of the manuscript.

Conflicts of interest

There are no conflicts to declare.

Acknowledgements

This work was financially supported by the National Key Research and Development Program of China (2023YFC3905300), the National Natural Science Foundation of China (22376080, 22306073, 22125606, and 22193051), and the Hubei Provincial Natural Science Foundation of China (2024AFA089).

Notes and references

1 S. Lin, X. Chen and Z. L. Wang, *Chem. Rev.*, 2022, **122**, 55209–55232.
2 C. Cai, B. Luo, Y. Liu, Q. Fu, T. Liu, S. Wang and S. Nie, *Mater. Today*, 2022, **52**, 299–326.
3 Z. Wang, A. Berbille, Y. Feng, S. Li, L. Zhu, W. Tang and Z. L. Wang, *Nat. Commun.*, 2022, **13**, 130.
4 Z. L. Wang, T. Jiang and L. Xu, *Nano Energy*, 2017, **39**, 9–23.
5 W. Xu, H. Zheng, Y. Liu, X. Zhou, C. Zhang, Y. Song, X. Deng, M. Leung, Z. Yang, R. X. Xu, Z. L. Wang, X. Zeng and Z. Wang, *Nature*, 2020, **578**, 392–396.
6 Z. Wang, X. Dong, W. Tang and Z. L. Wang, *Chem. Soc. Rev.*, 2024, **53**, 4349–4373.
7 J. Nie, Z. Ren, L. Xu, S. Lin, F. Zhan, X. Chen and Z. L. Wang, *Adv. Mater.*, 2020, **32**, 1905696.
8 S. Lin, L. Xu, A. Wang and Z. L. Wang, *Nat. Commun.*, 2020, **11**, 399.
9 C. Yun, S. Lee, J. Ryu, K. Park, J. Jang, J. Kwak and S. Hwang, *J. Am. Chem. Soc.*, 2018, **140**, 14687–14695.
10 Y. Xia, J. Li, Y. Zhang, Y. Yin, B. Chen, Y. Liang, G. Jiang and R. N. Zare, *Proc. Natl. Acad. Sci. U. S. A.*, 2023, **120**, e2302014120.
11 Y. Li, K. W. Kolasinski and R. N. Zare, *Proc. Natl. Acad. Sci. U. S. A.*, 2023, **120**, e2304735120.
12 B. Chen, Y. Xia, R. He, H. Sang, W. Zhang, J. Li, L. Chen, P. Wang, S. Guo, Y. Yin, L. Hu, M. Song, Y. Liang, Y. Wang, G. Jiang and R. N. Zare, *Proc. Natl. Acad. Sci. U. S. A.*, 2022, **119**, e2209056119.
13 S. Shaik, D. Danovich and R. N. Zare, *J. Am. Chem. Soc.*, 2023, **145**, 20132–20140.
14 J. Li, Y. Xia, X. Song, B. Chen and R. N. Zare, *Proc. Natl. Acad. Sci. U. S. A.*, 2024, **121**, e2318408121.
15 S. Jin, H. Chen, X. Yuan, D. Xing, R. Wang, L. Zhao, D. Zhang, C. Gong, C. Zhu, X. Gao, Y. Chen and X. Zhang, *JACS Au*, 2023, **3**, 1563–1571.
16 X. Yuan, D. Zhang, C. Liang and X. Zhang, *J. Am. Chem. Soc.*, 2023, **145**, 2800–2805.

17 S. Jin, R. Wang, H. Chen, X. Yuan and X. Zhang, *J. Phys. Chem. A*, 2023, **127**, 2805–2809.
18 X. Chen, Y. Xia, Z. Zhang, L. Hua, X. Jia, F. Wang and R. N. Zare, *J. Am. Chem. Soc.*, 2023, **145**, 21538–21545.
19 X. Chen, Y. Xia, Y. Wu, Y. Xu, X. Jia, R. N. Zare and F. Wang, *J. Am. Chem. Soc.*, 2024, **145**, 10868–10874.
20 L. Qiu and R. G. Cooks, *Angew. Chem., Int. Ed.*, 2022, **61**, e202210765.
21 J. Peng, K. Du, J. Sun, X. Yang, X. Wang, X. Zhang, G. Song and F. Feng, *Angew. Chem., Int. Ed.*, 2022, **62**, e202214991.
22 S. Pei, S. You, J. Ma, X. Chen and N. Ren, *Environ. Sci. Technol.*, 2020, **54**, 13333–13343.
23 Y. Wu, L. Bu, X. Duan, S. Zhu, M. Kong, N. Zhu and S. Zhou, *J. Clean. Prod.*, 2022, **273**, 123065.
24 C. Hu, Y. Chang, C. Yen, J. Chen, R. Muthukumaran and M. Chao, *Free Radicals Biol. Med.*, 2019, **143**, 193–202.
25 M. Han and M. Mohseni, *Water Res.*, 2020, **168**, 115169.
26 D. Xing, Y. Meng, X. Yuan, S. Jin, X. Song, R. N. Zare and X. Zhang, *Angew. Chem., Int. Ed.*, 2022, **61**, e202207587.
27 H. Baytekin, A. Patashinski, M. Branicki, B. Baytekin, S. Soh and B. Grzybowski, *Science*, 2011, **333**, 108–312.
28 Y. Sobolev, W. Adamkiewicz, M. Siek and B. Graybowski, *Nat. Phys.*, 2022, **18**, 1347–1355.